



Experimental and theoretical examination of the energy performance and CO₂ emissions of room air conditioners utilizing natural refrigerant R290 as a substitute for R22

Sharmas Vali Shaik¹ · Kirankumar Gorantla² · Saboor Shaik³ · Asif Afzal⁴ · Ali A. Rajhi⁵ · Erdem Cuce^{6,7}

Received: 16 July 2022 / Accepted: 10 December 2022 / Published online: 9 January 2023
© Akadémiai Kiadó, Budapest, Hungary 2023

Abstract

The purpose of this research is to analyze the performance of an air conditioner that uses natural refrigerant R290 both analytically and experimentally. The feasibility of R290 for R22 air conditioner is examined thoroughly. Since the alternatives used in R22 air conditioners possess high GWPs and they are controlled by the Kyoto Protocol. The Kyoto Protocol mainly indicates that the high GWP refrigerants used in refrigeration and air conditioning sectors are classified into one among the targeted greenhouse gases. Therefore, the present work focuses on ecofriendly-refrigerant R290 as a substitute to R22. In comparison to R22, R290 has no ODP and a very low GWP. An analytical study is conducted based on the actual VCR cycle. An experimental study was conducted on the R22 air conditioner with R290 at various outdoor conditions. Test results revealed that electrical energy consumption of air conditioner with R290 was 12.30% lower compared to R22 for the lower operating conditions and it was 11.40% lower compared to R22 for the higher operating conditions. Cooling capacity of R290 compared to R22 is lower in the range of 6.37–9.24% for the test conditions studied. For the operating circumstances studied, the energy efficiency ratio of R290 is higher than R22, ranging from 2.41 to 6.77%. Compressor discharge temperature of R290 is lower in the range of 8.67–15.32 °C for all the investigated conditions. When compared to R22, CO₂ emissions from air conditioners operating with R290 are lower in the range from 13.10 to 14.18%. The study revealed that R290 is a viable option to replace R22 used in air conditioners in terms of performance and environmental aspects.

Keywords Cooling capacity · CO₂ emissions · Energy efficiency ratio · GWP · R22 alternative refrigerants

List of symbols

A_{cs}	Cross sectional area (m ²)	h	Specific enthalpy (kJ kg ⁻¹)
BP	Boiling point (°C)	h_f	Liquid enthalpy (kJ kg ⁻¹)
D	Diameter (m)	h_{fg}	Enthalpy of vapourization (kJ kg ⁻¹)
DBT	Dry bulb temperature (°C)	h_1	Specific enthalpy at compressor inlet (kJ kg ⁻¹)
E_{An}	Annual Energy consumption (kWh)	h_2	Specific enthalpy at compressor outlet (kJ kg ⁻¹)
G	Mass flux (kg m ⁻² s ⁻¹)	h_4	Specific enthalpy at evaporator entry (kJ kg ⁻¹)
		L	Length (m)

✉ Saboor Shaik
saboor.nitk@gmail.com

✉ Asif Afzal
asif.afzal86@gmail.com

¹ Department of Mechanical Engineering, Srinivasa Ramanujan Institute of Technology (Autonomous), Ananthapuramu, Andhra Pradesh 515701, India

² Department of Humanities and Basic Sciences, Aditya College of Engineering, Surampalem, Andhra Pradesh 533437, India

³ School of Mechanical Engineering, Vellore Institute of Technology, Vellore, Tamil Nadu 632014, India

⁴ University Centre for Research & Development, Department of Mechanical Engineering, Chandigarh University, India, Gharuan Mohali, India

⁵ Department of Mechanical Engineering, College of Engineering, King Khalid University, P.O. Box 394, 61413 Abha, Saudi Arabia

⁶ Low/Zero Carbon Energy Technologies Laboratory, Faculty of Engineering and Architecture, Recep Tayyip Erdogan University, Zihni Derin Campus, 53100 Rize, Turkey

⁷ Department of Mechanical Engineering, Faculty of Engineering and Architecture, Recep Tayyip Erdogan University, Zihni Derin Campus, 53100 Rize, Turkey

m	Mass charge (kg)
\dot{m}	Mass flow rate of refrigerant (kg s^{-1})
MW	Molecular weight (kg kmol^{-1})
n	Polytropic index (dimensionless)
P	Pressure (bar)
P_c	Critical pressure (MPa)
P_e	Evaporating pressure (MPa)
P_k	Condensing pressure (MPa)
P_r	Pressure ratio (dimensionless)
q	Heat flux (W m^{-2})
Q_c	Refrigeration capacity of the system (kW)
Q_{cc}	Cooling capacity (W)
RE	Refrigeration, effect (kJ kg^{-1})
Re	Reynolds, number (dimensionless)
S_{Life}	Service life of the device (years)
T_d	Discharge temperature ($^{\circ}\text{C}$)
T_e	Evaporating temperature ($^{\circ}\text{C}$)
T_k	Condensing temperature ($^{\circ}\text{C}$)
T_s	Suction temperature ($^{\circ}\text{C}$)
V	Volume (m^{-3})
W_{ac}	Actual compressor work (kJ kg^{-1})
W_c	Isentropic compressor work (kJ kg^{-1})
WBT	Wet bulb temperature ($^{\circ}\text{C}$)

Abbreviations

CRT	Capacity rating test
DT	Domestic test
ET	Export test
DBT	Dry bulb temperature
HCFCs	Hydrochlorofluorocarbons
GWP	Global warming potential
ODP	Ozone depletion potential
TEWI	Total equivalent warming index
VCR	Vapour compression refrigeration
WBT	Web bulb temperature
HC	Hydrocarbon
HVAC	Heating, ventilation, and air conditioning

Greek letters

α_{recovery}	Recycling factor (Dimensionless)
β	Indirect emission factor ($\text{kg CO}_{2e} \text{ kWh}^{-1}$)
ΔP	Pressure drop (bar)
ΔP_e	Evaporator pressure drop (bar)
ΔP_f	Frictional pressure drop (bar)
ΔP_g	Gravitational pressure drop (bar)
ΔP_k	Condenser pressure drop (bar)
ΔP_m	Momentum pressure drop (bar)
ΔP_{tot}	Total pressure drop (bar)
η_c	Compression efficiency (%)
μ	Dynamic viscosity (Pa-s)
ρ	Density (kg m^{-3})
ρ_{11}	Vapour density at compressor inlet (kg m^{-3})

Subscripts

amb	Ambient
c	Critical
comp	Compressor
cond	Condenser
disch	Discharge
evap	Evaporator
f	Liquid phase
g	Vapour phase
i	Inside
in	Inlet
l	Liquid
m	Mixture
mea	Measured
o	Outside
out	Outlet
sub	Subcooling
suc	Suction
sup	Superheating
tot	Total
tpf	Two-phase friction

Introduction

In heat pump, refrigeration, and air conditioning systems, hydrochlorofluorocarbons (HCFCs) are extensively used because of their excellent thermophysical and thermodynamic characteristics. Because of the negative environmental impacts of HCFCs, the Montreal Protocol has decided to ban these HCFCs by 2030 in developed countries and by 2040 in developing countries [1–3]. The two most important concerns confronting the globe now are rising global warming and the depletion of the ozone layer of the atmosphere. As a result, the current work makes an effort to develop a more sustainable refrigerant with a lower global warming potential (GWP) and zero ozone depletion potential (ODP).

Natural refrigerants like hydrocarbons are becoming increasingly popular these days. These refrigerants are excellent for use in cooling systems as they have a very low GWP and no ODP. R290 is a hydrocarbon refrigerant that, despite its reputation as an explosive chemical substance, has no influence on the climate. R290 and other refrigerants were studied in the past to see if they could be used in place of R22. Testing was done on the refrigerants R134a, R290, and R407C to see how well they replaced R22 in HVAC systems and to determine their energy efficiency and irreversibility [4]. The mass distribution of R290 in a split air conditioner throughout the compressor start-up, during increased compressor speed, during the rise in refrigerant charge, and the shut-down time was studied experimentally by the Li et al. [5]. In the literature, a novel construction with a low pressure shell was described for minimizing the effect of leakage

on the performance of the R290 rolling piston compressor [6]. Singh et al. [7] conducted comparative study on cascade cooling system using natural refrigerant pairs. Study exhibited that R717-R290 refrigerant pair gives better performance in terms of economic and thermodynamic aspects. Ning et al. [8] did performance study on electric vehicles based on two-stage vapour compression air conditioning system operating with R290, R32, R454C and R410A.

Paradeshi et al. [9] conducted experimental exergy analysis of direct expansion solar assisted heat pump operating with R290 as a substitute to R22. The study exhibited that refrigerant R290 was an energy efficient compared to R22. Andrew Pon Abraham and Mohanraj [10] carried out performance study of automobile air conditioner operating with R430A as a substitute to R134a. The test results revealed that exergy destruction of air conditioner working with R430A was lower than R134a by 12–28%. Paradeshi et al. [11] performed exergy analysis of solar heat pump working with mixture refrigerant R433A as an alternative to R22. The investigation revealed that exergy destruction of heat pump operating with R433A was 8.1% lower compared to R22. Raveendran and Sekhar [12] carried out experimental performance study on refrigerator working with R134a and a hydrocarbon (HC) mixture (R290/R600a of 45.2%/54.8% by mass). The refrigerator was equipped with brazed plate heat exchanger as condenser. The study reported that exergy efficiency of HC mixture was 4 to 7% higher than R134a under analogous working conditions. Anand and Tyagi [13] carried out comprehensive experimental exergy analysis on 2 TR window air conditioner with various charges of R22 refrigerant. Experimental results shown that for 100% charged system, total exergy destruction was highest, whereas it was observed to be least when the system was charged with a 25%. Saravana kumar and selladurai [14] performed experimental investigation of exergy analysis on refrigerator with mixture R290/R600a as alternative to R134a. Researchers reported that COP of mixture refrigerant R290/R600a was 28.5% superior compared to R134a, whereas exergy efficiency of 38.6% and 42.1% were found at -10°C evaporator temperature for R134a and R290/R600a mixture, respectively.

The studies on the charge optimization of R290 in the split air-conditioner of R22 were carried out and reported a 35.5% as the optimum charge quantity [15]. Cold start-up characteristics were investigated for a R290 air-conditioner with rotary compressor experimentally and reported that higher start-up times for the pressures and the temperatures compared to R410A and R22 systems [16]. The explosion characteristics of R290 split air conditioner's indoor and outdoor units were studied and reported a maximum explosion pressure of 820 Pa for the indoor unit [17]. The simulation studies were carried out on automotive air-conditioning system with open piston compressor using R134a, R1234yf,

and R290 refrigerants [18]. The semi-empirical models were reported to be reliable for characterization parameters. R290 refrigerant migration characteristics were studied in a room air conditioner and it was reported that the dramatic and smooth change phases were dominated by mass and heat transfer, respectively [19]. Experimental investigations were carried out to study dynamic characteristics of an air-conditioning system with R290 rotary compressor and reported higher minimum suction pressure in warm start-up than the cold start-up and its performance under low ambient heating conditions was also carried out and reported a higher time to reach steady pressure conditions than R410A [20, 21].

Additionally, studies were done to determine the refrigerant distribution and leakage characteristics of R290 in split air-conditioning systems, and it was recommended that the solenoid valve be located near the capillary tube to minimize leakage and increase safety [22]. The effect of R290 refrigerant charge mass on the performance of split air-conditioning systems equipped with various expansion devices (capillary, thermostatic, and electronic expansion valves) was investigated, and it was concluded that a higher degree of superheat was required for optimal performance [23]. Fire hazard and leakage reduction studies on R290 air-conditioning systems were conducted, and it was recommended to install a solenoid valve near the capillary to eliminate the possibility of leakage and fire incidents [24].

Musharavati et al. [25] carried out detailed thermo-economic and thermodynamic assessment on biomass energy system for desalinated water production and power generation. Researchers also focused on the multiple objective optimizations using the multi-objective grey wolf optimizer (MOGWO) algorithm in order to obtain the optimal solution with the minimum amount of total cost rate and highest exergy efficiency. The study reported that the number of impacts of the distillation unit does not impact the carbon dioxide emissions. Alirahmi et al. [26] investigated the exergoeconomic and environmental analysis on novel solar heliostat integrated energy system. Researchers also conducted the multi-objective optimization using the multi-objective genetic algorithm in order to determine the minimum value of the cost rate and the maximum amount of exergetic efficiency. In this study, an artificial neural network (ANN) was employed as a mediator tool to speed up the optimization process.

The solubility of R290 in the oil of an air conditioner's rotary compressor was investigated, and a higher degree of superheat was recommended for the mineral oil to improve performance [27]. The refrigerant R290 was used as a replacement for R134a in experimental trials in a vending machine and performance of R290 was found to be superior to that of R134a [28]. According to a theoretical performance study, the performance of a binary combination (R1270/R290 of 80/20 by mass %) was similar to that of R22 [29]. The performance

of R290 was reported to be better than R22 in theoretical investigation, however R407C refrigerant would be a superior retrofit option for R22 [30].

From the literature, it is observed that the theoretical analysis of R290 based on actual VCR cycle is very much limited. In actual practice, pressure drops occur at various system components and these pressure drops will be different for each considered refrigerant. Moreover, theoretical computation of pressure drops of each individual refrigerant is not reported. Therefore, the present work finds an important research gap to do the analytical computation of pressure drops of different refrigerants and also to conduct the thermodynamic performance analysis of refrigerants based on actual (practical) VCR cycle. Furthermore, computation of polytropic index, specific power and CO₂ emissions of R22 air conditioner operating with R290 at various capacity rating tests (CRTs) have not been reported. As a result, the current research work focuses on both analytical and experimental performance investigation of window air conditioner operating with R22 and R290 at various test conditions.

The main originality of the present work is given below.

- In the present study, more realistic study is conducted based on actual VCR cycle.
- Pressure drops computation are not reported in the literature and hence, a novel contribution is added in terms of analytical computation of pressure drops occur in evaporator and condenser for each considered refrigerant.
- In this work, experimental performance and environmental impact parameters such as polytropic index, specific power and CO₂ emissions of R22 air conditioner operating with R290 at various capacity rating tests (CRTs) have been conducted.

Materials and methods

Properties (Physical, environmental and safety groups) of considered refrigerants like R22 and R290 were taken from ASHRAE data hand book and they are listed in Table 1 [31]. The saturation vapour pressure curves of refrigerants R22 and R290 are shown Fig. 1.

The saturation vapour pressure curves of R22 and R290 are depicted in Fig. 1. From Fig. 1, it is noticed that the saturation pressure of R290 is 9.6% lower than that of R22 in the temperature range of –30 to 70 °C, indicating that the refrigerant

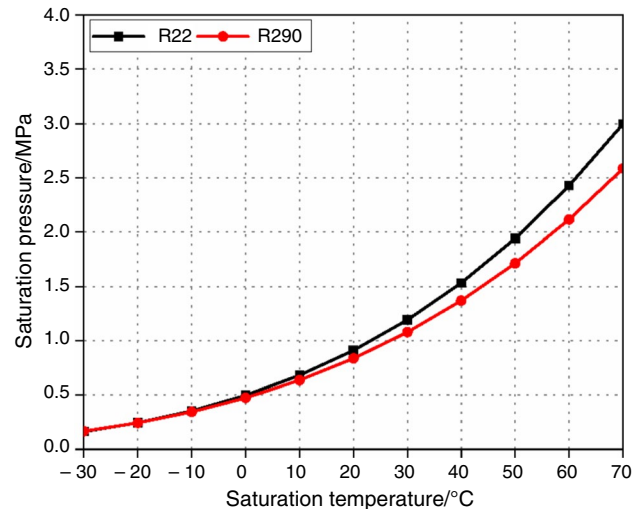


Fig. 1 Saturation temperature versus saturation pressure of refrigerants

R290 has similar properties and could be used as a substitute for R22.

Analytical study on computation of pressure drops in heat exchangers

There is a total pressure drop in condenser or evaporator that is made up of three different pressure drops: gravitational, frictional, and momentum pressure drops as shown in Eq. (1) [32–35].

$$\Delta P_{\text{tot}} = \Delta P_g + \Delta P_f + \Delta P_m \quad (1)$$

Gravitational pressure drop for horizontal tubes is zero and hence, total pressure drop in a heat exchanger can be computed using Eq. (2) [32–35].

$$\Delta P_{\text{tot}} = \Delta P_f + \Delta P_m \quad (2)$$

Mass flow rates of refrigerants are required before determining pressure drops in heat exchangers (condenser and evaporator). As a result, the thermodynamic analysis of an air conditioner is carried out using the operating circumstances listed in Table 2. Table 3 lists the features of a window air conditioner, while Fig. 4 displays its photographic aspect.

Table 1 Properties of refrigerants

Refrigerants	MW/kg k ⁻¹ mol ⁻¹	BP/°C	P_c /MPa	T_c /K	ASHRAE Safety class	ODP	GWP (100 years)
R22	86.46	-40.81	4.990	369.30	A1	0.055	1760
R290	44.09	-42.11	4.251	369.89	A3	0	3

Table 2 Designated Operating conditions of air conditioner [36]

Operating conditions	Values
Condensing temperature/°C	54.4
Condenser outlet temperature/°C	46.1
Subcooling/°C	8.3
Evaporating temperature/°C	7.2
Suction gas temperature/°C	18.3
Superheating/°C	11.1
Ambient Temperature Surrounding the Compressor/°C	35

Table 3 Specifications of R22 air conditioner

<i>Window air conditioner</i>	
Cooling capacity/W	4730
Power input/W	1475
Refrigerant	R22
<i>Condenser</i>	
Condenser type	Plate type finned tube condenser
Material	Copper
Tube diameter/mm	6.3
Length per tube/mm	790
Number of tubes	36
Width/mm	81
Height/mm	420
Fins per inch	14
Tube layout	Staggered arrangement
<i>Expansion device</i>	
Expansion device	Capillary tube
Refrigerant	R22
Material	Copper
Diameter/mm	1.63
Length/m	2.3
<i>Evaporator</i>	
Evaporator type	Plate type finned tube evaporator
Material	Copper
Tube diameter/mm	6.3
Length per tube/mm	440
Number of tubes	54
Width/mm	81
Height/mm	405
Fins per inch	14
Tube layout	Staggered arrangement
<i>Chamber dimensions</i>	
Indoor chamber dimensions	2.81 m long × 2.7 m wide × 2.16 m high
Outdoor chamber dimensions	2.85 m long × 2.7 m wide × 2.16 m high
Indoor chamber heater/W	1000
Outdoor chamber heater/W	1000

Frictional pressure drop in condenser

Müller-Steinhagen and Heck correlations have been demonstrated to be useful in estimating frictional pressure drop for condensing flow of various refrigerants inside tubes, and the relevant correlations are presented in Eqs. (3–8) [32, 37–39].

$$\Delta P_{\text{tpf}} = G_{11}(1-x)^{1/3} + Bx^3 \tag{3}$$

$$G_{11} = A + 2(B-A)x \tag{4}$$

$$A = (dP)_{f,l} = \frac{f_l LG^2}{2\rho_l d_i} \quad B = (dP)_{f,g} = \frac{f_g LG^2}{2\rho_g d_i} \tag{5}$$

The length of heat exchangers can be measured from air conditioner and it is 27 m for the condenser and 23.2 m for the evaporator, respectively.

$$f_l = \frac{64}{\text{Re}_l} f_g = \frac{64}{\text{Re}_g} \quad \text{for } \text{Re}_l, \text{Re}_g \leq 1187 \tag{6}$$

$$f_l = \frac{0.3164}{\text{Re}_l^{0.25}} f_g = \frac{0.3164}{\text{Re}_g^{0.25}} \quad \text{for } \text{Re}_l, \text{Re}_g > 1187 \tag{7}$$

$$\text{Re} = \frac{Gd_i}{\mu}; G = \frac{\dot{m}}{A_{cs}} \tag{8}$$

where *A* is a single-phase liquid pressure drop, *B* is a single-phase gas pressure drop. Müller-Steinhagen and Heck correlation can be used only if *Re*_l > 100 and *B* > *A*.

Momentum pressure drop in condenser

For condensing flows within tubes, the correlations used to compute the momentum pressure drop for different refrigerants are expressed in Eqs. (9–10) [32–35].

$$\Delta P_m = G^2 L \left[\frac{x^2}{\rho_g \alpha} + \frac{(1-x)^2}{\rho_l (1-\alpha)} \right] \tag{9}$$

$$\alpha = \frac{1}{1 + \left(\frac{1-x}{x}\right) \left(\frac{\rho_g}{\rho_l}\right)^{0.67}} \tag{10}$$

The dryness fraction (*x*) of the refrigerant is required to calculate frictional and momentum pressure reductions in the condenser, and so the refrigerant quality is adjusted from 0.99 to 0.01 in increments of 0.1 for theoretical calculations. Average pressure drop data are derived from these computations. Furthermore, it has been stated in the literature that complete condensing occurs at an integrated mean quality of 0.45 [40, 41]. The properties of

refrigerants are measured at condensing temperature in the two-phase zone (condensing zone) (T_k).

In the case of an evaporator, the refrigerant's dryness fraction (x) is computed using Eq. (11) [42].

$$(h_f)_{T_{ko}} = (h_f + xh_{fg})_{T_c} \tag{11}$$

Total pressure drop in condenser

In condenser, as the refrigerant decelerates during condensation, the momentum change in condenser is negative, which should result in pressure recovery unlike in evaporator and hence, total pressure drop in condenser is computed using Eq. (12) [35].

$$(\Delta P_{tot})_k = \Delta P_f - \Delta P_m \tag{12}$$

Frictional pressure drop in evaporator

From several literatures, it has been shown that Müller-Steinhagen and Heck correlation can be used to compute the frictional pressure drop for evaporating flows inside the tubes and the correlation is described in the section “[Frictional pressure drop in condenser](#)” [32, 37–39]. For the purpose of theoretical calculations of pressure drop, dryness fraction (x) of the refrigerant is varied from 0.01 to 0.99 in increments of 0.1 although it is computed from Eq. (11). Since, the Eq. (11) gives quality (x) of refrigerant entering into the evaporator.

Momentum pressure drop in evaporator

Chawla’s correlation is used to compute the momentum pressure drop for evaporating flows inside the tubes as shown in using Eqs. (13–18) [42].

$$\left(\frac{\Delta P}{\Delta L}\right)_M = \frac{4Gqx}{D_i h_{fg} \rho_f} \left[\left(1 - \frac{1}{\epsilon R_\rho}\right) \left(1 + \frac{1-x}{x} \epsilon\right) + \left(1 + \frac{1-x}{x \epsilon R_\rho}\right) (1 - \epsilon) \right] \tag{13}$$

$$(\Delta P)_M = \frac{4GLqx}{D_i h_{fg} \rho_f} \left[\left(1 - \frac{1}{\epsilon R_\rho}\right) \left(1 + \frac{1-x}{x} \epsilon\right) + \left(1 + \frac{1-x}{x \epsilon R_\rho}\right) (1 - \epsilon) \right] \tag{14}$$

$$\epsilon = 62 \left(\frac{1-x}{x R_\rho}\right) [Re_f Fr_f]^{-1/6} [R_\rho]^{-0.9} \tag{15}$$

$$Re_f = \frac{G(1-x)^2}{\mu_f} \tag{16}$$

$$Fr_f = G^2(1-x)^2 / (\rho_f^2 g D_i) \tag{17}$$

$$R_\rho = \rho_f / \rho_g; \quad R_\mu = \mu_f / \mu_g \tag{18}$$

Total pressure drop in evaporator

Total pressure drop occur in the evaporator can be estimated using Eq. (19) [32–35].

$$(\Delta P_{tot})_e = \Delta P_f + \Delta P_m \tag{19}$$

From the given room air conditioner, it is observed that refrigerant flowing in both heat exchangers is in parallel connection. Therefore, mass flow rates of refrigerants obtained from thermodynamic analysis can be halved and this could be taken into account for computing total pressure drop. The total pressure drop occurred in both heat exchangers (condenser and evaporator) is given in Table 4.

Table 4 Total pressure drops obtained for R22 and R290

Refrigerants	$\dot{m}/\text{kg s}^{-1}$	$\dot{m}_k/\text{kg s}^{-1}$ ($\dot{m}_k = \dot{m}/2$)	$G/\text{kg m}^{-2} \text{s}^{-1}$	Pressure drops occurred in condenser			
				x	$\Delta P_f/\text{bar}$	$\Delta P_m/\text{bar}$	$\Delta P_{tot}/\text{bar}$
R22	0.0299	0.0149	479.588	0.49	0.649	0.305	0.344
R290	0.01703	0.00851	273.157	0.49	0.491	0.224	0.267
Refrigerants	$\dot{m}/\text{kg s}^{-1}$	$\dot{m}_e/\text{kg s}^{-1}$ ($\dot{m}_e = \dot{m}/2$)	$G/\text{kg m}^{-2} \text{s}^{-1}$	Pressure drops occurred in evaporator			
				X	$\Delta P_f/\text{bar}$	$\Delta P_m/\text{bar}$	$\Delta P_{tot}/\text{bar}$
R22	0.0299	0.0149	479.588	0.49	1.482	0.00152	1.483
R290	0.01703	0.00851	273.157	0.49	1.224	0.00136	1.225

Analytical computation of energy performance evaluation of air conditioner

Actual Vapour compression refrigeration (VCR) cycle is considered while assessing the thermodynamic performance of R22 alternatives. Actual VCR cycle’s P–h diagram is shown in Fig. 2 [43].

Assumptions considered in this work are given below [44–46].

- In a steady-state system, all processes are believed to be in a steady flow.
- Changes in kinetic and potential energy are not taken into account in the system components.
- Expansion is assumed to be isenthalpic.
- Heat losses and gains in the discharge and suction lines are not taken into account.
- Pressure losses in the discharge and suction lines are not taken into consideration.
- Pressure drops at the suction valve, discharge valve of the compressor are neglected.
- Pressure drops that occurred in both evaporator and condenser are computed as described in section “Analytical study on computation of pressure drops in heat exchangers”
- Isentropic efficiency of compressor for R22 alternatives is computed as given in Eq. (23)

Thermodynamic performance characteristics of alternative refrigerants are computed using Eqs. (20–30) [42, 44, 47, 48].

(i) Mass flow rate of refrigerant is estimated as [42, 44, 47].

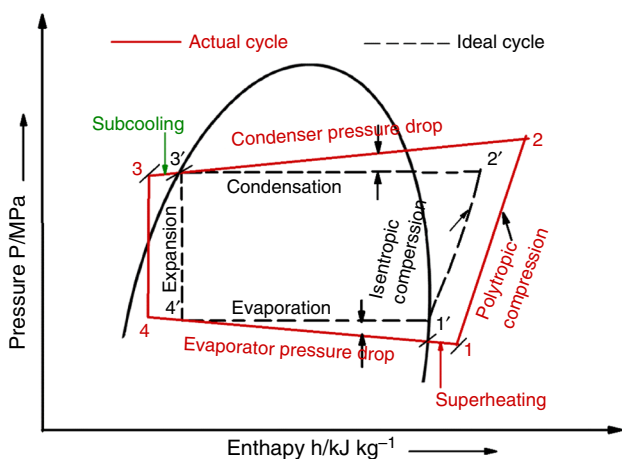


Fig. 2 P–h diagram of actual VCR cycle

$$\dot{m} = \frac{Q_c}{RE} = \frac{Q_c}{(h_1 - h_4)} \tag{20}$$

(ii) Refrigeration effect is evaluated as [42, 44, 47].

$$RE = (h_1 - h_4) \tag{21}$$

(iii) compressor work is calculated as [42, 44, 47].

$$W_c = (h_2 - h_1) \tag{22}$$

(iv) Isentropic efficiency of compressor for alternative refrigerants is computed as [48].

$$\eta_c = 0.976695 - 0.0366432 \left(\frac{P_k}{P_e} \right) + 0.0013378 \left(\frac{P_k}{P_e} \right)^2 \tag{23}$$

(v) Actual compressor work is estimated as [42, 44, 47].

$$W_{ac} = \frac{(h_2 - h_1)}{\eta_c} \tag{24}$$

(vi) Power input to compressor is evaluated as [42, 44, 47].

$$P_{comp} = \frac{\dot{m}W_c}{\eta_c} = \frac{\dot{m}(h_2 - h_1)}{\eta_c} = \dot{m}W_{ac} \tag{25}$$

(vii) Energy efficiency ratio (EER) of air conditioner is given by [42, 44, 47].

$$EER = (RE/W_{ac}) \tag{26}$$

(viii) Pressure ratio is given by [42, 44, 47].

$$P_r = (P_k/P_e) \tag{27}$$

(ix) The temperature of the compressor discharge is calculated using refrigerant superheated property tables and interpolation for the specified degree of superheat corresponding to the entropy difference [42].

(x) Specific power or power per ton of refrigeration (PPTR) is computed as [42, 47].

$$PPTR = \left(\frac{3.5167W_{ac}}{RE} \right) = \left(\frac{3.5167}{COP} \right) \tag{28}$$

(xi) Volumetric refrigeration capacity is given by [42, 47].

$$VRC = (\rho_1 \times RE) = (\rho_1 \times (h_1 - h_4)) \tag{29}$$

(xii) Polytropic indexes of various refrigerants are computed from the following relation [42, 47].

$$T_d = T_e \left(\frac{P_k}{P_e} \right)^{\frac{n-1}{n}} \quad (30)$$

Analytical results obtained from the thermodynamic performance evaluation of R22 and R290 are presented in Table 5.

From Table 5, it is evident that natural refrigerant propane (R290) performs better than R22 in terms of energy and thermodynamic performance aspects. However, because R290 is a flammable refrigerant, precautions must be taken when conducting experiments, as indicated in section “Safety precautions for R290”.

Validation of analytical results

The performance parameters of R22 and R290 are computed using a MATLAB program devised in this study. The program's results have been compared to those found in the literature [44]. Arora et al. (2007) carried out theoretical study on actual VCR cycle operating with R22 alternatives. Operating conditions such as T_e of 7 °C, T_k of 50 °C, superheating and subcooling of 5 °C, condenser and evaporator pressure loss of 0.1 and 0.2 bar and compressor efficiency of 75%, respectively, were considered by the authors in their study. In the present MATLAB code, same operating conditions are taken for the purpose of validation. The deviations attained in code compared with researcher results are given in Table 6.

From Table 6, it is evident that present work results exhibit good agreement with literature results and deviations

attained are within $\pm 1.9\%$. Therefore, the present MATLAB code developed in this research work is treated as persuasive.

Experimental

The experimental setup consists of calibrated room type calorimeter, which includes two weather simulation chambers of equal size separated by a non-weather stripped composite wall. The walls of the chambers are constructed with materials (asbestos sheet, plywood, polystyrene and standard air gap) with those mentioned in Indian Standards as per the specifications given in the IS-1391 Part-1 (1992). Each indoor and outdoor simulation chambers are provided with a small wooden chamber for the circulation of air. Dimensions of chambers are given in Table 3. Both the chambers are equipped with instrumented reconditioning equipments such as split air conditioners, psychrometers, relative humidity sensors, temperature sensors, heater coils and steam-injecting nozzles which are connected to the steam riser kept outside the chambers whose output may be measured and controlled to counterbalance the room side (indoor side) dehumidifying and cooling effect and the outdoor side humidifying and heating effect of the unitary air conditioner under test. The schematic diagram of experimental test setup for testing the performance of air conditioner is shown in Fig. 3.

Test air conditioner

The test air conditioner, which is a residential window room air conditioner of capacity 4.73 kW, is placed between

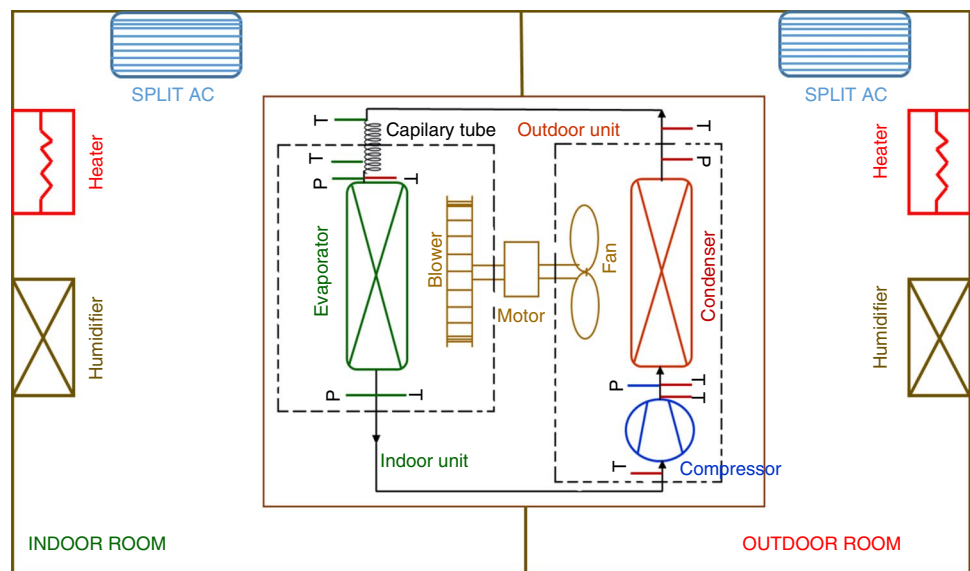
Table 5 Thermodynamic performance characteristics of R22 and R290

Refrigerants	$\dot{m}/\text{kg s}^{-1}$	RE/kJ kg ⁻¹	$W_{ac}/\text{kJ kg}^{-1}$	EER	W_{cp}/kW	PPTR/kW TR ⁻¹	
R22	0.03056	154.756	48.489	3.191	1.482	1.102	
R290	0.01762	268.397	82.787	3.242	1.458	1.084	
Refrigerants	P_k/MPa	P_e/MPa	P_r	$\eta_c/\%$	n	$T_d/^\circ\text{C}$	VRC/kJ m ⁻³
R22	2.1806	0.4771	4.570	83.71	1.197	90.28	2950
R290	1.9099	0.4651	4.106	84.87	1.157	70.71	2545

Table 6 Comparison of present work results with Arora et al. (2007) results [44]

Performance parameters	Arora et al. (2007) results for R22	Present code results for R22	Deviation/%	Arora et al. (2007) results for R410A	Present code results for R410A	Deviation/%
Refrigeration effect/kJ kg ⁻¹	155.60	154.604	-0.64	154.40	153.049	-0.87
Actual compressor work/kJ kg ⁻¹	40.320	40.302	-0.04	43.020	43.432	0.95
COP	3.860	3.836	-0.62	3.590	3.523	-1.86

Fig. 3 Schematic diagram of experimental facility used to test a room air conditioner



indoor and outdoor simulation chambers as shown in Fig. 3. It is modified using copper tubing for mounting the various sensors like pressure and temperature sensors. The arrangement has been made to adopt a flow meter, stagnation temperature and stagnation pressure sensors at the outlet of the evaporator and also at the outlet of the compressor. The arrangement is done such that any component of the air conditioner (such as compressor, evaporator, condenser and capillary tube) can be removed without loss of refrigerant. The photographic view of test air conditioner is depicted in Fig. 4.

Experimentation

The room air conditioner was mounted on the test bed. While handling the system, care was taken against mechanical damages. By suitable means, it was ensured that there was no air leakage from one chamber (indoor side or outdoor side) to the other. The psychrometers were located in both the indoor and outdoor chambers. The wet bulb thermometer tip was kept wet all the time. Controlling the dehumidifiers, air heaters and humidifiers did the reconditioning of the air in both the chambers and maintained the CRT conditions as per IS 1391 Part 1 (1992). After confirming the steady state for an hour, temperatures of air (dry bulb and wet bulb) in both indoor chamber and outdoor chambers were recorded for an hour at an interval of 10 min. Power input to the compressor, refrigerant pressures and temperatures at various system components were recorded. In the present research work, experiments on air conditioner working with R22 and R290 are carried out for both domestic market conditions as well as for export market conditions as described in the IS 1391 Part 1 (1992) and test conditions are given in Table 7



Fig. 4 Photographic view of the test room air conditioner

[49]. The details of instruments used in the experimentation are given in Table 8.

From Table 7, it is noticed that operating conditions (CRT-DT and CRT-ETA) are categorized into lower operating conditions, whereas CRT-ETB is classified into higher operating conditions for the purpose of comparison.

Safety precautions for R290

R290 is a flammable refrigerant and therefore, the following safety measures should be taken while charging flammable refrigerants [50].

- (i) All the joints and electrical connections probable to spark should be sealed properly.
- (ii) The room should be ventilated well before starting the air conditioner in order to prevent any augmentation of flammable refrigerant.

Table 7 Standard test conditions of air conditioner [49]

Type of test	Indoor side conditions		Outdoor side conditions	
	DBT/°C	WBT/°C	DBT/°C	WBT/°C
Capacity rating test for domestic market (CRT-DT)	27	19	35	30
CRT for export test conditions A (CRT-ETA)	27	19	35	24
CRT for export test conditions B (CRT-ETB)	29	19	46	24

Table 8 Instruments used in the present experimental work

Name of Instrument	Specifications and range	Accuracy
Thermocouples (K-type)	– 55 to 125 °C	± 0.5 °C
Pressure transducers	0 bar to 35 bar	± 0.25% FSO
Mass flow meter (Coriolis type)	0.003 to 0.09 kg s ⁻¹	± 0.2%
Power transducer	0–5 kW	± 10 W
Platform type electronic weighing machine	0–25 kg	± 2 g

(iii) Particularly designed leak detectors used for flammable refrigerants should be placed in the room.

(iv) A fire extinguisher should be provided in the area where flammable refrigerant cylinders are stored.

(v) The air conditioner unit should be properly labelled specifying that the refrigerant contained is flammable in nature so that it indicates alertness to the worker.

(vi) When flammable refrigerant needs to be removed from the air conditioner, it should be done outside.

Experimental performance analysis of air conditioner

Performance characteristics such as cooling capacity, power consumption, energy efficiency ratio, pressure ratio, polytropic index, discharge temperature of compressor, specific power and TEWI are computed experimentally for all the investigated test conditions and they are presented in results and discussion section.

The cooling capacity of air conditioner is calculated by using the following equation [42, 48].

$$Q_{cc} = \dot{m}(h_{\text{evap,out}} - h_{\text{evap,in}}) \quad (31)$$

In the Eq. (31), refrigerant enthalpies were calculated based on pressure and temperature measurements at the evaporator outlet and the condenser liquid line for $h_{\text{evap,out}}$ and $h_{\text{evap,in}}$, respectively. Compressor power consumption is obtained from experiments. Similarly, parameters such as temperatures and pressures at inlet and outlet of system components are measured experimentally.

Energy efficiency ratio (EER) of air conditioner is computed as [42, 48]

$$\text{EER} = \frac{Q_{cc}}{P_{\text{comp}}} \quad (32)$$

Experimental polytropic indexes of R22 and R290 are computed from the following relation [47].

$$T_d = T_s \left(\frac{P_{\text{disch}}}{P_{\text{suc}}} \right)^{\frac{n-1}{n}} \quad (33)$$

The experimental observations recorded for R22 and R290 for various test conditions are given in Table 9.

CO₂ emission analysis of air conditioner

Total equivalent warming index (TEWI) is used to analyse the CO₂ emissions released from air conditioner.

$$\begin{aligned} \text{TEWI} &= \text{Direct CO}_2 \text{ emissions} + \text{Indirect CO}_2 \text{ emissions} \\ &= [(GWP_{100} \times L \times S_{\text{Life}}) + ((GWP_{100} \times m(1 - \alpha_{\text{recovery}}))] \\ &\quad + [(E_{\text{An}} \times S_{\text{Life}} \times \beta)] \end{aligned} \quad (34)$$

TEWI analysis of R22 and R290 is carried out with some assumptions as presented below [43, 51, 52]. Operating period of an apparatus (air conditioner) is 12 h/d; refrigerant leakage rate is 7% per year; service life of the apparatus is 15 years; indirect emission factor (β) is 0.82 kg CO_{2e} kWh⁻¹; recycling or recovery factor (α_{recovery}) is 0.75. For Indian climatic conditions, the indirect emission factor (β) was reported in the literature, and it is about 0.82 kg CO_{2e} kWh⁻¹ [53].

The quantity of refrigerant charge required can be computed from Eq. (35) empirical correlation [46].

Table 9 Experimentally measured data of R22 and R290 for various operating conditions

Measured parameters	Type of tests for R22			Type of tests for R290		
	CRT-DT	CRT-ETA	CRT-ETB	CRT-DT	CRT-ETA	CRT-ETB
Indoor room DBT/°C	27.36	27.65	29.63	26.81	27.54	29.67
Indoor room WBT/°C	18.67	19.41	19.67	19.45	19.65	19.36
Outdoor room DBT/°C	35.45	35.65	46.67	35.56	35.72	46.54
Outdoor room WBT/°C	29.5	24.63	24.65	29.67	24.72	24.65
Compressor suction pressure (P_{suc} /bar)	6.23	6.22	6.43	5.90	5.87	6.21
Compressor discharge pressure (P_{disch} /bar)	22.82	22.98	27.72	19.95	20.02	25.43
Condenser outlet pressure ($P_{cond,out}$ /bar)	22.01	22.17	26.76	19.28	19.33	24.69
Pressure drop in condenser (ΔP_k /bar)	0.81	0.81	0.96	0.67	0.69	0.74
Evaporator inlet pressure ($P_{evap,in}$ /bar)	6.56	6.57	6.81	6.11	6.12	6.56
Evaporator outlet pressure ($P_{evap,out}$ /bar)	6.23	6.22	6.43	5.90	5.87	6.21
Pressure drop in evaporator (ΔP_e /bar)	0.33	0.35	0.38	0.21	0.25	0.35
Pressure ratio ($P_r = P_{suc}/P_{disch}$)	3.663	3.694	4.311	3.381	3.410	4.095
Compressor power consumption (P_{comp} /W)	1545	1572	1729	1355	1380	1532
Compressor suction temperature (T_{suc} /°C)	24.30	25.33	29.33	21.86	22.32	25.50
Compressor discharge temperature (T_d /°C)	82.18	82.87	94.48	66.86	67.69	85.81
Condenser outlet temperature ($T_{cond,out}$ /°C)	50.63	51.88	61.06	50.77	52.13	65.42
Evaporator inlet temperature ($T_{evap,in}$ /°C)	6.56	6.70	7.15	6.97	6.86	7.05
Evaporator outlet temperature ($T_{evap,out}$ /°C)	18.29	18.14	16.92	18.22	18.27	18.78
Mass flow rate (\dot{m} /kg s ⁻¹)	0.03285	0.03278	0.03346	0.01613	0.01594	0.01565
Refrigeration effect (RE/kJ kg ⁻¹)	138.975	136.474	115.448	265.043	261.150	224.010
Polytropic index (n)	1.158	1.155	1.154	1.132	1.131	1.150

$$m = \frac{2}{3}\rho_{Cond}V_{Cond} + \frac{1}{3}\rho_{Evap}V_{Evap} \tag{35}$$

From specifications of system components as shown in Table 3, charge quantity obtained for R290 using Eq. (35) is 386 g whereas mass of refrigerant R22 contained in the present air conditioner is 800 g. From the above discussion, it is evident that, mass charge required for R290 is 51.7% lower compared to R22 and hence, R290 alleviates direct CO₂ emissions. For an instance, TEWI analysis of R290 and R22 for domestic test conditions is given in Table 10.

Results and discussion

Cooling capacity

When performing trials with alternative refrigerants, cooling capacity is regarded as a critical parameter. If the cooling

capability of an alternative refrigerant differs significantly from that of the baseline fluid, the compressor must be fully modified, which is an expensive investment. As a result, if an alternative refrigerant provides similar cooling capability to the baseline candidate, that refrigerant can be regarded as a feasible substitute.

Figure 5a, b show the cooling capacity and cooling capacity deviations of refrigerant R290 when compared to R22 under various operating situations. Figure 5a shows that the cooling capacity of a pure hydrocarbon refrigerant R290 is lower than that of R22 because its vapour specific volume is greater than R22 and hence mass flow rate decreases, lowering R290's cooling capacity.

From Fig. 5a, it is noticed that for lower operating conditions (CRT-DT and CRT-ETA), cooling capacity obtained for R22 is 4.565 kW and 3.863 kW for the higher operating conditions (CRT-ETB). Experimental results revealed that cooling capacity of R290 is 6.37% lower compared to R22 for the lower operating conditions and it is 9.24%

Table 10 TEWI of air conditioner operating with R22 and R290 for domestic test conditions

Refrigerants	Mass charge/kg	Direct CO ₂ emissions/kg CO _{2e}	Indirect CO ₂ emissions/kg CO _{2e}	TEWI/kg CO _{2e}
R22	0.8	1830.4	83,235.33	85,065.73
R290	0.386	1.505	72,999.27	73,000.77

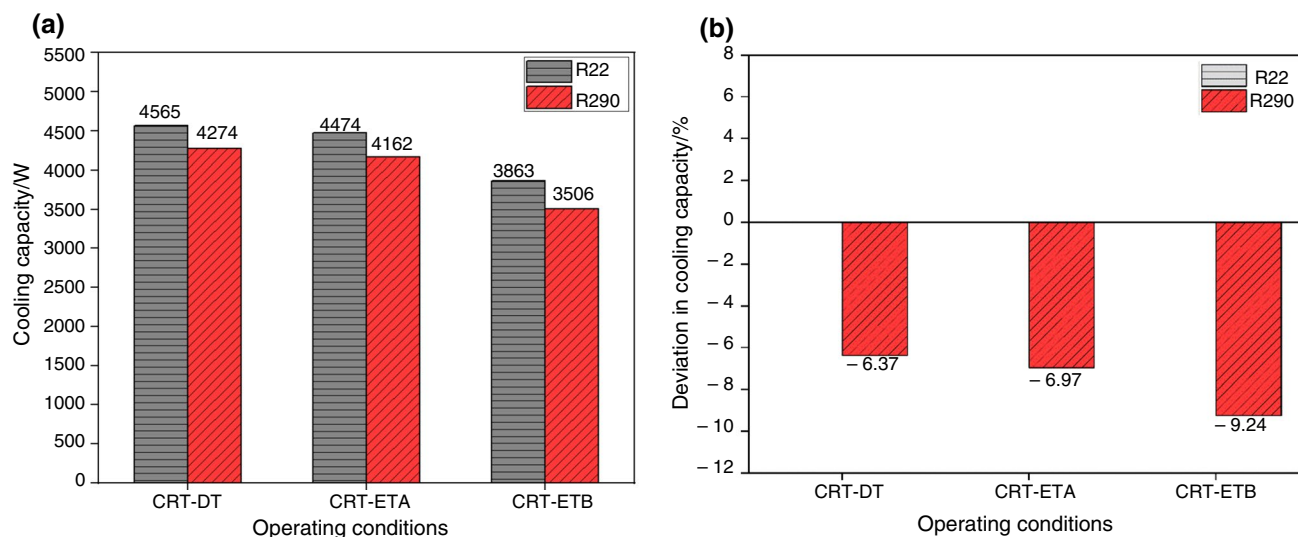


Fig. 5 Cooling capacities of refrigerants: **a** comparison, **b** deviation

lower compared to R22 for the higher operating conditions as shown in Fig. 5b. This is due to lower volumetric capacity of R290 compared to R22 and hence, R290 requires moderately higher size of compressor compared to R22. However, for higher operating conditions, cooling capacities of R22 and R290 are lower with similar variations as presented in Fig. 5a.

The variations in cooling capacities for CRT-DT and CRT-ETA are within the experimental error range and moreover, Devotta et al. [54] reported similar type of deviations in cooling capacities of R22 and R290 under lower operating conditions (CRT-DT and CRT-ETA).

Compressor power

Figure 6A, b shows the compressor power consumption and deviations in compressor power of hydrocarbon refrigerant R290 as compared to R22 for various investigated operating conditions. Figure 6a shows that the compressor power consumption of R290 is lower than R22 for all of the investigated operating conditions. This is due to its lower pressure ratio compared to R22. From Fig. 6a, it is observed that for lower operating conditions, power consumed by the compressor for R22 is 1.545 kW and 1.729 kW for the higher operating conditions.

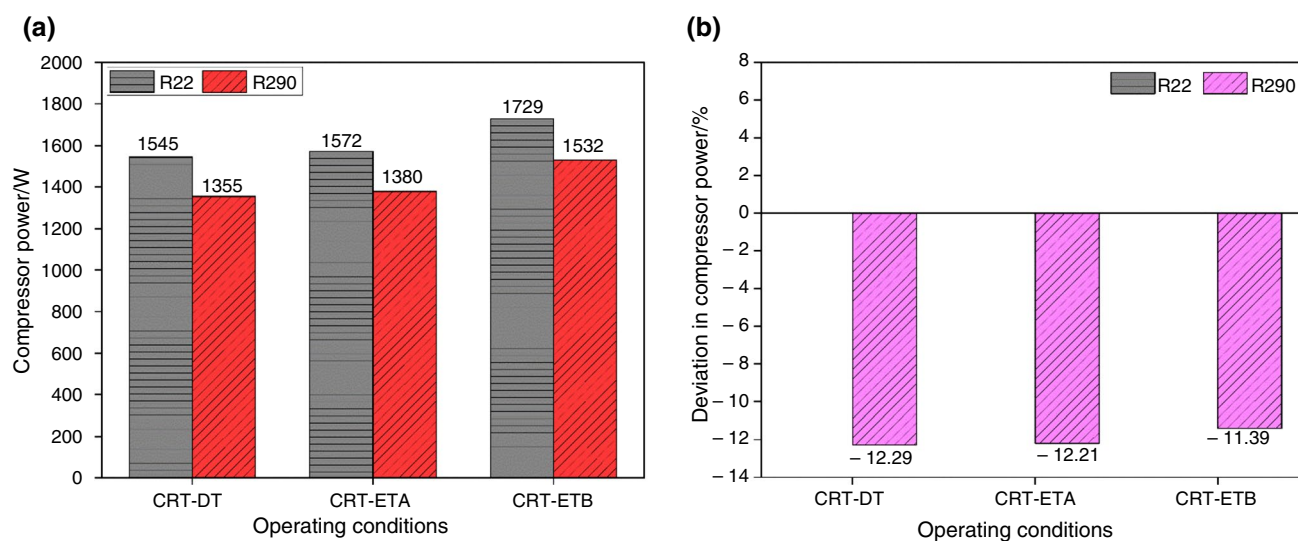


Fig. 6 Compressor power of pure refrigerants: **a** comparison, **b** deviation

Test results revealed that the compressor power consumption of R290 is 12.29% lower compared to R22 for the lower operating conditions and it is 11.39% lower compared to R22 for the higher operating conditions as shown in Fig. 6b.

Pressure drops in heat exchangers

In actual practice, pressure drops occur in heat exchangers (evaporator and condenser) that will significantly affect the performance of air conditioner. Hence, it is essential to consider these pressure drops while evaluating the performance of the system. The condenser and evaporator pressure drops are obtained from the experiments. Figure 7 represents

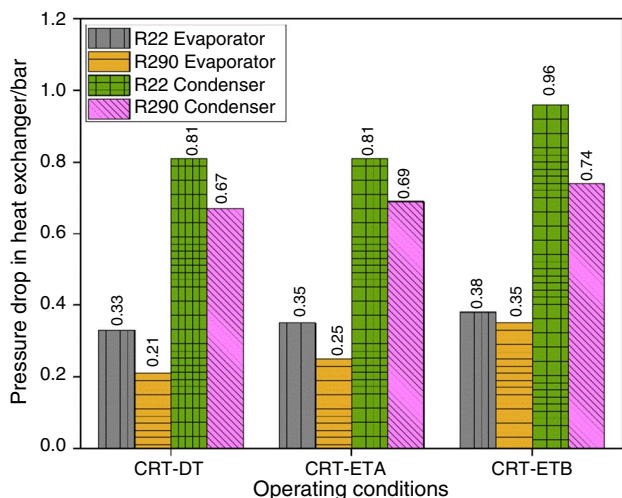


Fig. 7 Pressure drops in heat exchangers operating with R22 and R290

the pressure drops occurred in condenser and evaporator. From Fig. 7, it is observed that for all the investigated operating conditions, the pressure drops in the evaporator and condenser obtained for R22 are higher than R290. This is due to lower mass flow rate, density and viscosity of R290 compared to R22. Furthermore, pressure drops occurred in evaporator and condenser depends on the thermophysical properties of refrigerants.

Test results revealed that evaporator pressure drop of R290 is 12.29% lower compared to R22 for the lower operating conditions and it is 11.39% lower compared to R22 for the higher operating conditions. On the other hand, pressure drop obtained in condenser for R290 is lower in the range from 17.2 to 22.9% compared to R22 for the operating tests conducted.

Energy efficiency ratio (EER)

EER is a measure of a device's performance index when it is charged with a specific refrigerant. Figure 8a, b depicts the EER and deviation in EER of R290 as compared to R22 for various investigated operating conditions. From Fig. 8a, it is noticed that for lower operating conditions, EER obtained for R22 is 2.954 and 2.234 for the higher operating conditions. Similarly, from Fig. 8a, it is also evident that EER of R290 is higher for all the investigated operating conditions when compared to R22. This is due to its lower energy consumption of compressor.

The reduction in EERs at higher operating conditions for the investigated refrigerants (R22 and R290) are due to increase in condenser temperatures that causes the reduction in cooling capacities as well as increase in power

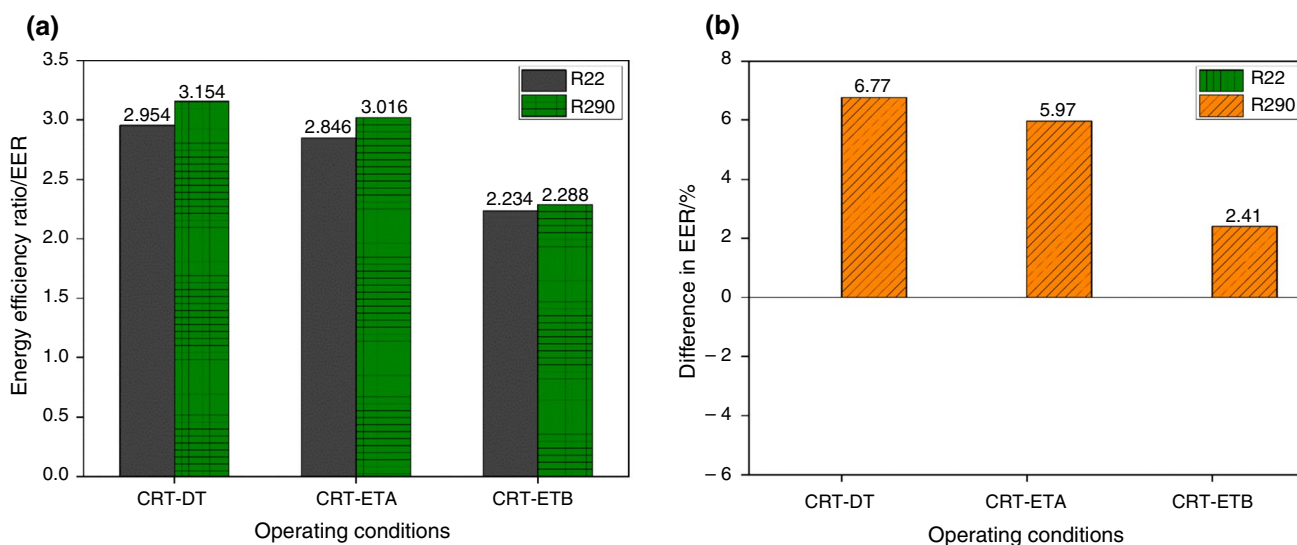


Fig. 8 EERs of refrigerants: a comparison, b deviation

consumptions by the compressor. Hence, EERs of refrigerants decrease at higher operating conditions.

Experimental results exhibit that EER of air conditioner working with R290 is 6.77% higher compared to R22 for the lower operating conditions and it is 2.41% higher compared to R22 for the higher operating conditions as represented in Fig. 8b.

Specific power

Specific power denotes the energy consumption for a unit refrigeration capacity of a given system when it is charged with a specific refrigerant. Specific power is inversely proportional to energy efficiency ratio (EER) which in turn depends on cooling capacity as well as compressor power. Higher the specific power, the lower will be the EER and vice versa. Figure 9a, b illustrates the specific power and deviation in specific power of refrigerant R290 as compared to R22 for various investigated operating conditions. From Fig. 9a, it is noticed that for lower operating conditions, specific power obtained for R22 is 1.190 kW/TR and 1.574 kW/TR for the higher operating conditions. Experimental results reveal that specific power of air conditioner working with R290 is 6.31% lower compared to R22 for the lower operating conditions and it is 2.35% lower compared to R22 for the higher operating conditions. This is due to higher EER of R290.

Pressure ratio

Pressure ratio is the ratio of discharge pressure to the suction pressure of compressor. Pressure ratio depends upon thermodynamic properties of refrigerants. Figure 10a, b exhibits the

pressure ratios and deviation in pressure ratio of refrigerant R290 as compared to R22 for various investigated operating conditions. From Fig. 10a it is clear that the pressure ratio of R290 is lower than R22 for all of the investigated operating situations. This is due to the lower discharge and suction pressure of R290 compared to R22. Lower pressure ratio of refrigerant is advantageous in terms of lower compressor power consumption and lower compressor discharge temperature.

From Fig. 10a, it is observed that for lower operating conditions, pressure ratio of compressor for R22 is 3.663 and it is 4.311 for the higher operating conditions. Experimental test results revealed that pressure ratio of compressor operating with R290 is 7.69% lower compared to R22 for the lower operating conditions and it is 5.01% lower for the higher operating conditions.

Polytropic index and compressor discharge temperature

Figure 11A exhibits the polytropic index of refrigerants R22 and R290. From Fig. 11a, it is evident that polytropic index of R290 is lower for all the investigated operating conditions when compared to R22. This is due to the effect of thermodynamic properties of refrigerant on polytropic index. Refrigerant with lower polytropic index is beneficial from the viewpoint of lower compressor discharge temperature.

From Fig. 11a, it is observed that for lower operating conditions, polytropic index of R22 is 1.158 and it is 1.154 for the higher operating conditions. The polytropic index of R290 was found to be lower in the range of 0.34–2.24% for all operating conditions investigated when compared to R22.

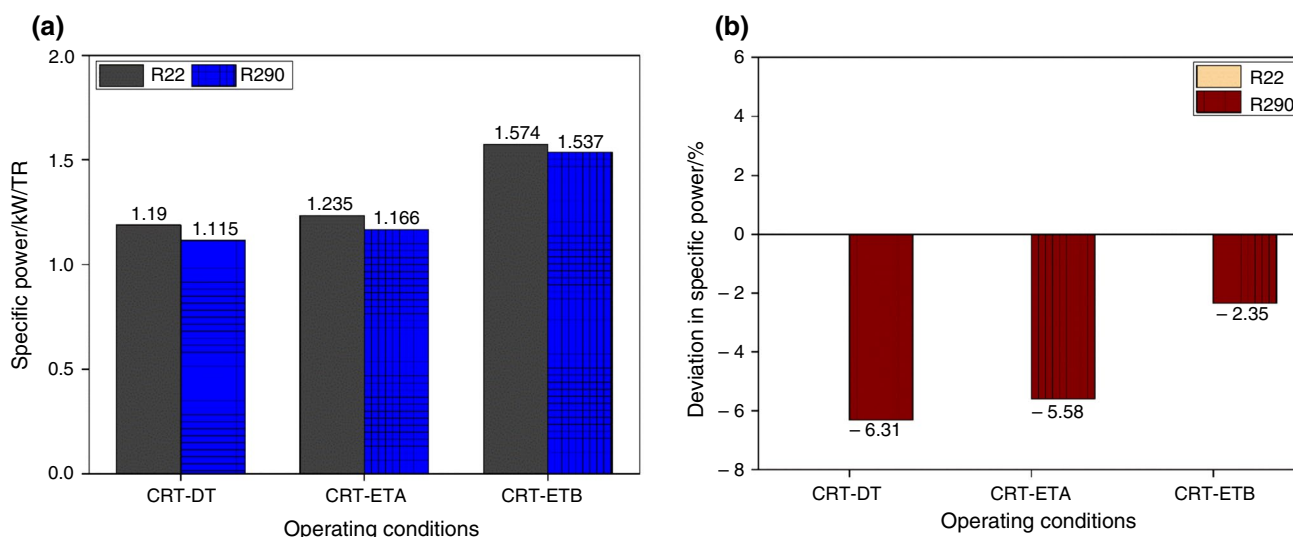


Fig. 9 Specific power of refrigerants: a comparison, b deviation

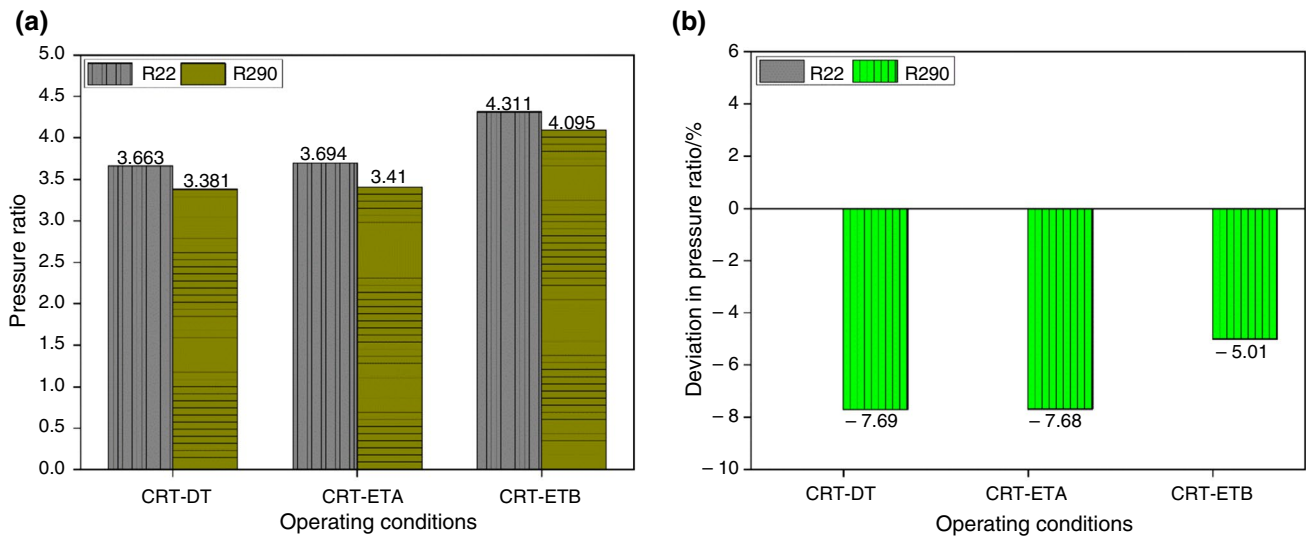


Fig. 10 Pressure ratios of refrigerants: a comparison, b deviation

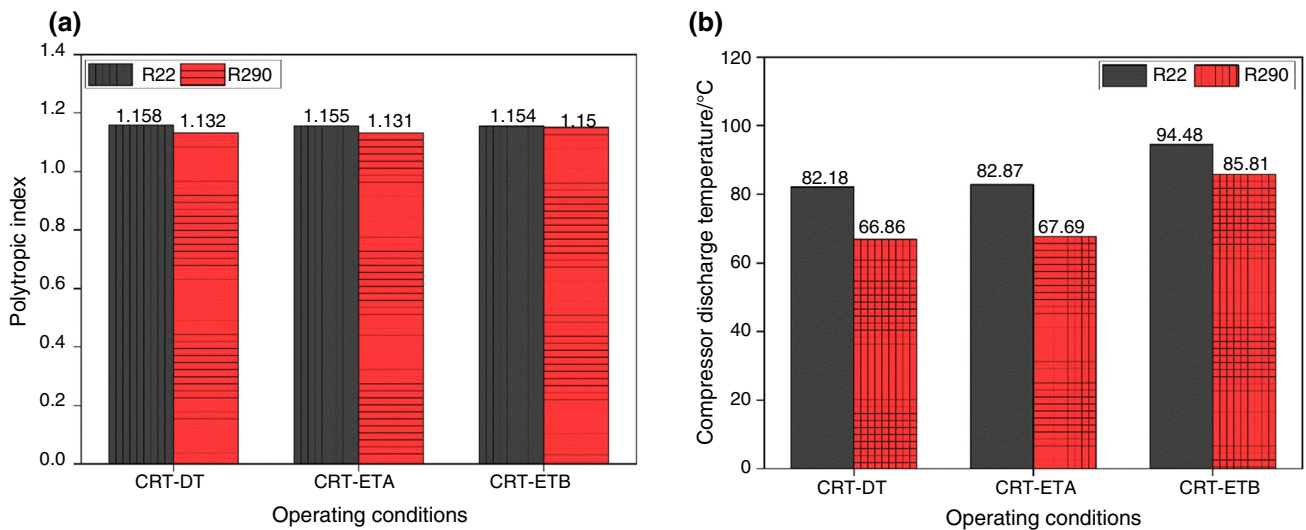


Fig. 11 a Polytropic index of refrigerants, b compressor discharge temperature of refrigerants

While employing alternative refrigerants, the compressor lifetime and reliability of the system as well as the stability of refrigerant and lubricant should be considered. These parameters can be examined by measuring the compressor discharge temperature of refrigerants. Compressor discharge temperature depends on pressure ratio and polytropic index of the given refrigerant. Refrigerant with higher discharge temperature causes the deterioration of lubricant characteristics and refrigerant stability and also causes the burnt out of motor windings of the compressor and thus, it decreases the compressor lifetime and stability [55]. As a result, compressor discharge temperature should be kept as low as feasible in order to maximize compressor lifetime and stability.

Figure 11b depicts the compressor discharge temperatures of refrigerants (R22 and R290) for various investigated operating conditions. From Fig. 11b, it is noticed that for lower operating conditions, discharge temperature obtained for R22 is 82.18 °C and 94.48 °C for the higher operating conditions. Figure 11b further shows that the compressor discharge temperature of R290 is lower for all of the investigated operating conditions than R22. This is because it has a lower pressure ratio and polytropic index than R22.

Test results revealed that compressor discharge temperature of R290 is 15.32 °C lower compared to R22 for the lower operating conditions and it is 8.67 °C lower compared to R22 for the higher operating conditions.

Therefore, refrigerant R290 exhibits greater stability and lifetime of compressor.

Total equivalent warming index (TEWI)

Total equivalent warming index (TEWI) is used to analyse CO₂ emissions from air conditioners operating with various refrigerants. Figure 12 exhibits the TEWI of refrigerants studied. From Fig. 12, it is evident that TEWI (both direct and indirect CO₂ emissions) of R290 is lower for all the investigated operating conditions when compared to R22. This is due to its lower energy consumption of compressor and lower GWP. Refrigerant with lower TEWI is beneficial from the viewpoint of lower global warming and sustainable environment.

From Fig. 12, it is observed that for lower operating conditions, CO₂ emissions (TEWI) of air conditioner working with R22 is 85065 kgCO_{2e} and it is 94978 kgCO_{2e} for the higher operating conditions. The TEWI of R290 is lower in the range of 13.10–14.18% under all operating situations compared to R22, according to test data.

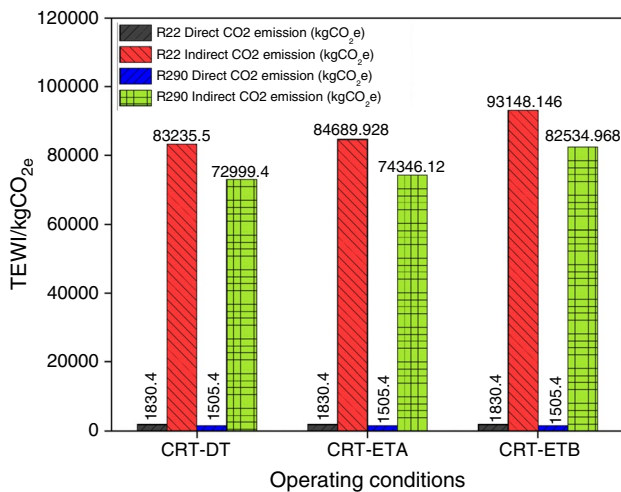


Fig. 12 TEWI of refrigerants

Table 11 Comparison between experimental and theoretical performance results of R22 and R290

Refrigerants	Parameters	Theoretical	Experimental	Deviation (%)
R22	Cooling capacity/W	4730	4565	-3.48
	Compressor power/W	1482	1545	4.25
	EER	3.191	2.954	-7.42
R290	Cooling capacity/W	4730	4274	-9.64
	Compressor power/W	1458	1355	-7.06
	EER	3.242	3.154	-2.71

Comparison of present experimental performance results of refrigerants with analytical performance results

In the present work, experimental performance results obtained for R22 and R290 have been compared with that of analytical performance results. The deviations obtained between experimental and theoretical performance results of R22 and R290 are given in Table 11.

UNCERTAINTY ANALYSIS

Uncertainty is used to denote a potential value that an error in the measurement might have. Let W_{ER} be the experimental result of uncertainty and W₁, W₂, W₃, W_n be the uncertainties in the independent variables. While various independent variables are used in the function ‘ER’ then the distinct terms are combined by the method of root sum square which is expressed as follows [56, 57].

$$W_{ER} = \sqrt{\left(\frac{\partial ER}{\partial Y_1} W_1\right)^2 + \left(\frac{\partial ER}{\partial Y_2} W_2\right)^2 + \dots + \left(\frac{\partial ER}{\partial Y_n} W_n\right)^2} \tag{36}$$

For example, cooling capacity is a function of mass flow rate and refrigeration effect which in turn depends on enthalpies of refrigerant. Enthalpy quantities are determined from the thermodynamic properties of refrigerants with respect to the measured pressure and temperature values. Hence, the source of uncertainty is in the measurement of pressure and temperature. Similarly, uncertainty source could be identified while doing uncertainty analysis of other performance parameters. Uncertainty equations for the performance parameters are given below [56, 57].

Coefficient of performance (COP) is given as

$$COP = \frac{Q_{cc}}{P_{comp}} \tag{37}$$

$$Q_{cc} = \dot{m}(RE) = \dot{m}(h_{evap,out} - h_{evap,in}) \tag{38}$$

$$Q_{cc} = f(\dot{m}, RE) \tag{39}$$

Table 12 Uncertainty in experimental performance parameters of R22 and R290

Refrigerants	Performance parameters	Uncertainty/% for various operating conditions		
		CRT-DT	CRT-ETA	CRT-ETB
R22	Cooling capacity ($\delta Q_{CC}/W$)	± 1.96	± 1.94	± 1.88
	Power consumption ($\delta P_{comp}/W$)	± 1.37	± 1.32	± 1.12
	COP ($\delta COP/W$)	± 2.40	± 2.35	± 2.20
	Compressor discharge temperature ($\delta T_d/^\circ C$)	± 1.35	± 1.31	± 1.10
R290	Cooling capacity ($\delta Q_{CC}/W$)	± 1.64	± 1.62	± 1.49
	Power consumption ($\delta P_{comp}/W$)	± 1.18	± 1.16	± 1.01
	COP ($\delta COP/W$)	± 2.03	± 2.01	± 1.85
	Compressor discharge temperature ($\delta T_d/^\circ C$)	± 1.16	± 1.14	± 1.0

$$RE = f(P_{evap,out}, T_{evap,out}, P_{cond,out}, T_{cond,out}) \quad (40)$$

$$[\cdot: h_{evap,in} = h_{cond, out}]$$

observed that uncertainties in all the considered performance parameters are within 2.50%.

$$\left(\frac{\delta RE}{RE}\right) = \sqrt{\left(\frac{\delta P_{evap,out}}{P_{evap,out}}\right)^2 + \left(\frac{\delta T_{evap,out}}{T_{evap,out}}\right)^2 + \left(\frac{\delta P_{cond,out}}{P_{cond,out}}\right)^2 + \left(\frac{\delta T_{cond,out}}{T_{cond,out}}\right)^2} \quad (41)$$

$$\left(\frac{\delta Q_{cc}}{Q_{cc}}\right) = \sqrt{\left(\frac{\delta \dot{m}}{\dot{m}_{mea}}\right)^2 + \left(\frac{\delta RE}{RE}\right)^2} \quad (42)$$

Compressor power consumption (P_{comp}) is expressed as

$$P_{comp} = f(P_{comp,mea}, T_{suc}, T_d, P_{suc}, P_{disch}, T_{amb}) \quad (43)$$

$$\left(\frac{\delta P_{comp}}{P_{comp}}\right) = \sqrt{\left(\frac{\delta P_{comp}}{P_{comp,mea}}\right)^2 + \left(\frac{\delta T_{suc}}{T_{suc}}\right)^2 + \left(\frac{\delta T_d}{T_d}\right)^2 + \left(\frac{\delta P_{suc}}{P_{suc}}\right)^2 + \left(\frac{\delta P_{disch}}{P_{disch}}\right)^2 + \left(\frac{\delta T_{amb}}{T_{amb}}\right)^2} \quad (44)$$

$$COP = f(Q_{cc}, P_{comp}) \quad (45)$$

$$\left(\frac{\delta COP}{COP}\right) = \sqrt{\left(\frac{\delta Q_{cc}}{Q_{cc}}\right)^2 + \left(\frac{\delta P_{comp}}{P_{comp}}\right)^2} \quad (46)$$

Compressor discharge temperature (T_d) is expressed as

$$T_d = f(T_{d,mea}, T_{suc}, P_{suc}, P_{disch}, T_{amb}) \quad (47)$$

$$\left(\frac{\delta T_d}{T_d}\right) = \sqrt{\left(\frac{\delta T_d}{T_{d,mea}}\right)^2 + \left(\frac{\delta T_{suc}}{T_{suc}}\right)^2 + \left(\frac{\delta P_{suc}}{P_{suc}}\right)^2 + \left(\frac{\delta P_{disch}}{P_{disch}}\right)^2 + \left(\frac{\delta T_{amb}}{T_{amb}}\right)^2} \quad (48)$$

Conclusions

The present investigation focuses on energy performance analysis and CO₂ emission analysis of residential unitary R22 air conditioner operating with sustainable refrigerant R290 at various capacity rating test conditions. The conclusions drawn from this investigation are given below.

- For each investigated refrigerant, the frictional pressure drop, momentum pressure drop, and total pressure drop occurred in heat exchangers (condenser and evaporator) were calculated analytically.
- Analytical results revealed that R290's EER was 1.45% higher than that of R22. Similarly, R290 outperforms R22 in terms of pressure ratio, discharge temperature, specific power, and other performance characteristics.
- Experiments on the energy performance of air conditioner with R22 and R290 were carried out under vari-

Uncertainties in performance characteristics of air conditioner operating with R22 and R290 at various test conditions are given in Table 12. From Table 12, it is

ous test conditions. The energy consumption of an air conditioner operating with R290 was reduced by 11.39 to 12.29% when compared to compared to R22 for all the

- test conditions studied. Similarly, energy efficiency ratio (EER) of R290 was 2.41–6.77% higher than that of R22.
- Experimental polytropic index of R290 was 1.132, whereas R22 has polytropic index of 1.158. Similarly, pressure ratio of R290 was 3.381, whereas R22 has pressure ratio of 3.663. Due to lower pressure ratio and polytropic index of R290, its compressor discharge temperature decreases and it was 8.67–15.32 °C lower compared to R22.
 - CO₂ emissions (TEWI) of air conditioner working with R290 was 14.18% lower compared to R22 for the lower operating conditions and it was 13.10% lower for the higher operating conditions. Global warming potential of R290 was very much lower (98.3%) compared to that of R22.
 - Charge quantity required for air conditioner operating with R290 was 51.75% lower compared to R22 and hence, R290 alleviates the direct CO₂ emissions into atmosphere.
 - From both analytical and experimental study, it was observed that the performance of refrigerant R290 was better compared to R22 in terms of energy of savings and environmental aspects and hence, R290 can be regarded a more environment friendly alternative to R22, which is commonly used in domestic window air conditioners.
 - The present work can be carried out extensively in near future by optimizing the refrigerant charge quantity and capillary lengths of R22 and R290.

Acknowledgements The author extend his appreciation to the Deanship of Scientific Research at King Khalid University for funding this work through research groups program under grant number R.G.P. 2/129/43.

Author contributions SVS contributed to Investigation, Methodology, Writing—review & editing. KG contributed to Conceptualization, Formal analysis, Writing—original draft, Writing—review & editing. SS contributed to Conceptualization, Formal analysis, Writing—review & editing. AA contributed to Conceptualization, Writing—original draft, Writing—review & editing. AAR contributed to formal analysis, supervision, Writing—review & editing. EC contributed to Writing—review & editing, supervision.

Declarations

Conflict of interest All authors declare that they have no conflict of interest.

References

1. UNEP, Montreal Protocol on substances that deplete the ozone layer Final Act, United Nation Environment Program, New York, USA, 1997.
2. Mohanraj M, Jayaraj S, Muraleedharan C. Environment friendly alternatives to halogenated refrigerants-A review. *Int J Greenh Gas Control*. 2009;3(1):108–19.
3. Powell RL. CFC phase-out: have we met the challenge. *J Fluor Chem*. 2002;114(2):237–50.
4. Padmanabhan VMV, Palanisamy SK. Exergy efficiency and irreversibility comparison of R22, R134a, R290 and R407C to replace R22 in an air conditioning system. *J Mech Sci Technol*. 2013;27(3):917–26.
5. Li T, Lu J, Chen L, He D, Qiu X, Li H, Liu Z. Measurement of refrigerant mass distribution within a R290 split air conditioner. *Int J Refrig*. 2015;57:163–72.
6. Wu J, Chen A. A new structure and theoretical analysis on leakage and performance of an oil-free R290 rolling piston compressor. *Int J Refrig*. 2015;49:110–8.
7. Singh KK, Kumar R, Gupta A. Comparative energy, exergy and economic analysis of a cascade refrigeration system incorporated with flash tank (HTC) and a flash intercooler with indirect sub cooler (LTC) using natural refrigerant couples. *Sustain Energy Technol Assess*. 2020;39:100716.
8. Ning Q, He G, Xiong G, Sun W, Song H. Operation strategy and performance investigation of a high-efficiency multifunctional two-stage vapor compression heat pump air conditioning system for electric vehicles in severe cold regions. *Sustain Energy Technol Assess*. 2021;48:101617.
9. Paradeshi L, Srinivas M, Jayaraj S. Thermodynamic analysis of a direct expansion solar-assisted heat pump system working with R290 as a drop-in substitute for R22. *J Therm Anal Calorim*. 2019;136(1):63–78.
10. Andrew Pon Abraham JD, Mohanraj M. Thermodynamic performance of automobile air conditioners working with R430A as a drop-in substitute to R134a. *J Therm Anal Calorim*. 2019;136(5):2071–86.
11. Paradeshi L, Mohanraj M, Srinivas M, Jayaraj S. Exergy analysis of direct-expansion solar-assisted heat pumps working with R22 and R433A. *J Therm Anal Calorim*. 2018;134(3):2223–37.
12. Raveendran PS, Joseph SS. Exergy analysis of a domestic refrigerator with brazed plate heat exchanger as condenser. *J Therm Anal Calorim*. 2017;127(3):2439–46.
13. Anand S, Tyagi SK. Exergy analysis and experimental study of a vapor compression refrigeration cycle: a technical note. *J Therm Anal Calorim*. 2012;110(2):961–71.
14. Saravanakumar R, Selladurai V. Exergy analysis of a domestic refrigerator using eco-friendly R290/R600a refrigerant mixture as an alternative to R134a. *J Therm Anal Calorim*. 2014;115(1):933–40.
15. Saravanan AL, Murugan RS, Lal DM. Investigations on charge reduction strategies to use R290 as an alternative to R22 in a split air conditioner. *Exp Heat Transfer*. 2017;30(2):126–38.
16. Wu J, Lin J, Zhang Z, Chen Z, Xie J, Lu J. Experimental investigation on cold startup characteristics of a rotary compressor in the R290 air-conditioning system under cooling condition. *Int J Refrig*. 2016;65:209–17.
17. Zhang W, Yang Z, Zhang X, Lv D, Jiang N. Experimental research on the explosion characteristics in the indoor and outdoor units of a split air conditioner using the R290 refrigerant. *Int J Refrig*. 2016;67:408–17.
18. Sotomayor PO, Parise JAR. Characterization and simulation of an open piston compressor for application on automotive air-conditioning systems operating with R134a, R1234yf and R290. *Int J Refrig*. 2016;61:100–16.
19. Jierong L, Tingxun L. Detailed dynamic refrigerant migration characteristics in room air-conditioner with R290. *Int J Refrig*. 2018;88:108–16.
20. Wu J, Lin J, Zhang Z, Chen Z, Xie J, Lu J. Experimental investigation of dynamic characteristics of a rotary compressor and its air conditioner using R290 during warm startup. *Appl Therm Eng*. 2017;125:1469–77.

21. Lin J, Wu J, Zhang Z, Chen Z, Xie J, Lu J. Experimental investigation of startup characteristics of R290 rotary compressor under low ambient temperature heating condition. *Int J Refrig*. 2017;77:128–35.
22. Tang W, He G, Cai D, Zhu Y, Zhang A, Tian Q. The experimental investigation of refrigerant distribution and leaking characteristics of R290 in split type household air conditioner. *Appl Therm Eng*. 2017;115:72–80.
23. Liu C, Wang D, Sun Z, Chen L, Shi J, Chen J. Effects of charge on the performance of R290 air conditioner with different expansion devices. *Appl Therm Eng*. 2018;140:498–504.
24. Tang W, He G, Sun W, Zhou S, Cai D, Zhu Y. Assessment of leakage and risk reduction of R290 in a split type household air conditioner. *Int J Refrig*. 2018;89:70–82.
25. Musharavati F, Khoshnevisan A, Alirahmi SM, Ahmadi P, Khanmohammadi S. Multi-objective optimization of a biomass gasification to generate electricity and desalinated water using Grey Wolf Optimizer and artificial neural network. *Chemosphere*. 2022;287:131980.
26. Alirahmi SM, Khoshnevisan A, Shirazi P, Ahmadi P, Kari D. Soft computing based optimization of a novel solar heliostat integrated energy system using artificial neural networks. *Sustain Energy Technol Assess*. 2022;50:101850.
27. Wu J, Chen Z, Lin J, Li J. Experimental analysis on R290 solubility and R290/oil mixture viscosity in oil sump of the rotary compressor. *Int J Refrig*. 2018;94:24–32.
28. Alkhaledi KA, Means K. A study on the use of propane (R-290) in vending machines as a substitute for R-134a to minimise the global warming potential. *Int J Global Warm*. 2018;14:131–41.
29. Dalkilic AS, Wongwises S. A performance comparison of vapour-compression refrigeration system using various alternative refrigerants. *Int Commun Heat Mass Transfer*. 2010;37(9):1340–9.
30. Devotta S, Waghmare AV, Sawant NN, Domkundwar BM. Alternatives to HCFC-22 for air conditioners. *Appl Therm Eng*. 2001;21:703–15.
31. ASHRAE, American Society of Heating Refrigeration and Air Conditioning Engineers Handbook-Fundamentals (SI), Atlanta, USA, 2017.
32. Didi MO, Kattan N, Thome JR. Prediction of two-phase pressure gradients of refrigerants in horizontal tubes. *Int J Refrig*. 2002;25(7):935–47.
33. Yin XW, Wang W, Patnaik V, Zhou JS, Huang XC. Flow Boiling Pressure Drop for R410A and RL32H in Multi-channel Tube. In: 16th international conference on refrigeration and air conditioning, Purdue, July 11–14, 2016.
34. Hirose M, Ichinose J, Inoue N. Development of the general correlation for condensation heat transfer and pressure drop inside horizontal 4 mm small-diameter smooth and microfin tubes. *Int J Refrig*. 2018;90:238–48.
35. Patel T, Parekh AD, Taylor PR. Experimental analysis of condensation heat transfer and frictional pressure drop in a horizontal circular mini channel. *Heat Mass Transf*. 2019;56:1579–600.
36. AHRI standard, Performance Rating of Positive Displacement Refrigerant Compressors and Compressor Units, Air Conditioning, Heating and Refrigeration Institute, Arlington, Virginia, 2015.
37. Shannak BA. Frictional pressure drop of gas liquid two-phase flow in pipes. *Nucl Eng Des*. 2008;238(12):3277–84.
38. Xu Y, Fang X. A new correlation of two-phase frictional pressure drop for evaporating flow in pipes. *Int J Refrig*. 2012;35(7):2039–50.
39. Xu Y, Fang X. A new correlation of two-phase frictional pressure drop for condensing flow in pipes. *Nucl Eng Des*. 2013;263:87–96.
40. Pate MB. Design considerations for air-conditioning evaporator and condenser coils. *Two-Phase Flow Heat Exchangers*. 1988;849–884.
41. Shah MM. A general correlation for heat transfer during film condensation inside pipes. *Int J Heat Mass Tran*. 1979;22(4):547–56.
42. Arora CP. Refrigeration and air conditioning. New York: Tata McGraw-Hill Education; 2009.
43. Joudi KA, Al-Amir QR. Experimental Assessment of residential split type air-conditioning systems using alternative refrigerants to R-22 at high ambient temperatures. *Energy Convers Manag*. 2014;86:496–506.
44. Arora A, Arora BB, Pathak BD, Sachdev HL. Exergy analysis of a vapour compression refrigeration system with R-22, R-407C and R-410A. *Int J Exergy*. 2007;4(4):441–54.
45. Cengel YA, Boles MA, Kanoglu M. Thermodynamics: an engineering approach. 9th ed. New York: McGraw-Hill Education; 2019.
46. Tian Q, Cai D, Ren L, Tang W, Xie Y, Liu F. An experimental investigation of refrigerant mixture R32/R290 as drop-in replacement for HFC410A in household air conditioners. *Int J Refrig*. 2015;57:216–28.
47. Arora RC. Refrigeration and air conditioning. New Delhi: PHI Learning Pvt. Ltd; 2012.
48. Al-Sayyab AKS, Navarro-Esbrí J, Mota-Babiloni A. Energy, exergy, and environmental (3E) analysis of a compound ejector-heat pump with low GWP refrigerants for simultaneous data center cooling and district heating. *Int J Refrig*. 2022;133:61–72.
49. Bureau of Indian Standards IS-1391 Part 1 Room air conditioners specification: Part 1 unitary air conditioners. New Delhi, India. 1992.
50. Colbourne D, Hühren R, Schrempf B, Ederberg L. Guidelines for the safe use of hydrocarbon refrigerants: A handbook for engineers, technicians, trainers and policy-makers-For a climate-friendly cooling. GIZ: Eschborn, Germany. 2012.
51. Bitzer Refrigerant report 20, Sindelfingen, Germany. Available at: https://www.bitzer-refrigerantreport.com/fileadmin/user_upload/A-501-20.pdf (2018).
52. Babu TP, Samaje VV, Rajeev R. Development of zero ODP, less TEWI, binary, ternary and quaternary mixtures to replace HCFC-22 in window air-conditioner. International Conference on Refrigeration and Air Conditioning, Purdue, July 17–20, 2006.
53. Bhawan S, Puram RK. CO₂ Baseline Database for the Indian Power Sector, Version 13. Government of India, Ministry of Power, Central Electricity Authority. 2018.
54. Devotta S, Padalkar AS, Sane NK. Performance assessment of HC-290 as a drop-in substitute to HCFC-22 in a window air conditioner. *Int J Refrig*. 2005;28(4):594–604.
55. Raj MH, Lal DM. A comparative study on the performance of a R22 window air conditioner retrofitted with R407C/R290/R600a refrigerant mixture. *Int J Ambient Energy*. 2008;29(4):207–17.
56. Moffat RJ. Describing the uncertainties in experimental results. *Exp Therm Fluid Sci*. 1988;1(1):3–17.
57. Holman JP. Experimental methods for engineers. 8th ed. New York: McGraw-Hill; 2012.

Publisher's Note Springer Nature remains neutral with regard to jurisdictional claims in published maps and institutional affiliations.

Springer Nature or its licensor (e.g. a society or other partner) holds exclusive rights to this article under a publishing agreement with the author(s) or other rightsholder(s); author self-archiving of the accepted manuscript version of this article is solely governed by the terms of such publishing agreement and applicable law.